

Delayed Enrichment by Unseen Galaxies: Explaining the Rapid Rise in IGM CIV Absorption from $z = 6-5$

R. H. Kramer ^{*1}, Z. Haiman ^{†2}, and P. Madau ^{‡3}

¹ *Institute for Astronomy, ETH Zurich, Wolfgang-Pauli-Strasse 27, CH-8093 Zurich, Switzerland*

² *Department of Astronomy, Columbia University, 550 West 120th Street, New York, NY 10027, USA*

³ *Department of Astronomy and Astrophysics, University of California Santa Cruz, 1156 High Street Santa Cruz, CA 95064, USA*

ABSTRACT

In the near future, measurements of metal absorption features in the intergalactic medium (IGM) will become an important constraint on models of the formation and evolution of the earliest galaxies, the properties of the first stars, and the reionization and enrichment of the IGM. The first measurement of a metal abundance in the IGM at a redshift approaching the epoch of reionization already offers intriguing hints. Between $z = 5.8$ and 4.7 (a 0.3 Gyr interval only 1 Gyr after the big bang), the measured density of C IV absorbers in the IGM increased by a factor of ~ 3.5 (Ryan-Weber et al. 2009; Becker, Rauch & Sargent 2009). If these values prove to be accurate, they pose two puzzles: (1) The total amount of C IV at $z = 5.8$ implies too little star formation to reionize the IGM by $z = 6$ or to match the *WMAP* electron scattering optical depth (τ). (2) The rapid growth from $z \approx 6-5$ is faster than the buildup of stellar mass or the increase in the star formation rate density over the same interval. We show that a delay of $\sim 0.4-0.7$ Gyr between the instantaneous production of ionizing photons and the later production of metal absorption features (added to the delay due to stellar lifetimes) can provide the full explanation for both puzzles. We calculate the delay in metal production due to finite stellar lifetimes alone and find that it is too short to explain the rapid C IV density increase. The additional delay could naturally be explained as the result of ~ 200 km/s outflows carrying carbon to distances of ~ 100 kpc, the typical distance between galaxies and C IV absorbers in enrichment simulations, and the typical outflow or absorption region scale observed at $z \approx 2-3$.

Key words: galaxies: formation – galaxies: high-redshift – intergalactic medium – cosmology: theory – quasars: absorption lines – dark ages, reionization, first stars.

1 INTRODUCTION

Most of the star formation taking place during the reionization epoch remains invisible to current observations, and a large fraction may remain invisible even to the *James Webb Space Telescope (JWST)* (e.g. Salvaterra, Ferrara & Dayal 2010). This unobserved population of faint galaxies must have contributed most of the high-energy photons that reionized the intergalactic medium (IGM). The ionization state of the intergalactic medium is one important probe of this population. Other constraints are provided by the detection of luminous Lyman-break galaxies (LBGs) and Lyman- α emitters (LAEs) at $z > 6$ (e.g. Bouwens et al. 2010; Tilvi et al. 2010). Although the directly observed population cannot account for all of the photons necessary

to reionize the IGM (and especially to match the *WMAP* Thompson-scattering optical depth from free electrons τ , Bolton & Haehnelt 2007; Oesch et al. 2009), they constrain the high-luminosity end of the galaxy luminosity function (LF).

The distribution (by element, in time, and in space) of the elements synthesised in these early generations of stars and subsequently expelled into the IGM (or incorporated into low-mass stars still observable in the local universe) will become an important source of information about the epoch of reionization in the near future. Currently the highest-redshift measurements of metal abundance in the IGM come from searches for C IV absorption features in quasar spectra (Ryan-Weber et al. 2009; Becker, Rauch & Sargent 2009).

The uncertainties on the $z \gtrsim 5$ C IV measurements are still large, but if the values prove to be accurate then they pose two puzzles. First, Ryan-Weber et al. (2009) find that the total amount of C IV at $z = 5.8$ implies too little star formation to reionize the IGM by $z = 6$. Second, Becker et al.

* Zwicky Fellow, ETH Zurich, roban.kramer@phys.ethz.ch

† zoltan@astro.columbia.edu

‡ pmadau@ucolick.org

(2009) find that the fractional increase in C IV density is larger than either the buildup of stellar mass or the increase in the star formation rate density (SFRD) over the same interval.

We show here that both puzzles can be solved by a delay between the production of ionizing photons and the enrichment of the IGM with the associated metals. In the next section (§2), we discuss current observations and models of C IV in the IGM in more detail. Section 3 presents our simple framework for modelling reionization and enrichment based on a galaxy luminosity function history.¹ In Section 4, we show that we can match reionization (§4.1) and enrichment constraints at a single redshift (§4.2) with simple models and physically plausible parameters, then go on to show that a delay of 0.4–0.7 Gyr (in addition to the delay due to finite stellar lifetimes) can produce the observed rapid rise in C IV absorber density (§4.3). In Section 5, we propose two explanations for the delay involving galactic outflows, and suggest observational tests of those explanations. In Section 6, we summarise our results and discuss how future observations and models will improve our understanding of early metal enrichment and reionization.

2 EXISTING OBSERVATIONS AND MODELS

Observations of absorption features in high-redshift quasar spectra are beginning to probe the IGM metallicity at redshifts approaching $z = 6$ (arguably close to the final stages of reionization). Currently the highest-redshift measurements are of the C IV 1548.2, 1550.8 Å doublet, redshifted into the near infrared (NIR). Ryan-Weber et al. (2009) identified three (plus one tentative) C IV features in a search between $z = 5.2$ and 6.2 along lines of sight to 9 quasars with a combined absorption distance of $\Delta X = 25.1$.² Becker et al. (2009) performed a similar search in four sight lines ($\Delta X = 11.3$), finding no absorption features. This is particularly surprising since their observations were sensitive to even lower column densities than Ryan-Weber et al. (2009), and therefore would have been expected to detect more C IV features per unit absorption distance if the column-density distribution followed the declining power-law form found at lower redshift.

Converting the absorption feature detections to the average C IV density in the IGM (expressed as a fraction of the critical density), and correcting for their completeness limits in column density, Ryan-Weber et al. (2009) found

$$\Omega_{\text{C IV}}(\langle z \rangle = 5.76) = (5.0 \pm 3.0) \times 10^{-9}. \quad (1)$$

¹ The full compendium of code and ancillary files needed to reproduce the present paper is available from the first author. Cosmological calculations were made with the COSMOLOGY package. The ENRICHPY package encapsulates our enrichment model. These resources are available at <http://www.astro.phys.ethz.ch/kramer/>, <http://roban.github.com/CosmoPy/>, and <http://roban.github.com/EnrichPy/>.

² ΔX is defined so that objects with constant comoving density and physical cross section have constant density per unit ΔX (Tyson 1988; Ryan-Weber et al. 2009).

Applying similar corrections to observations by Pettini et al. (2003), they found

$$\Omega_{\text{C IV}}(\langle z \rangle = 4.69) = (17 \pm 6) \times 10^{-9}. \quad (2)$$

The errors are still large on these measurements. If the $z = 5.76$ value is revised toward the upper end of the allowed range, then the puzzle of the rapid evolution in C IV will be greatly reduced (see Figure 4 in §4). However we will proceed here under the assumption that the central values are essentially correct. We therefore seek to resolve the puzzle of the rapid C IV growth.

The C IV density in the IGM is approximately constant at $\Omega_{\text{C IV}} \sim 2 \times 10^{-8}$ from $z = 2$ –4 (Ryan-Weber et al. 2009; Songaila 2001), a surprising result given that this is a period of intense star formation. Models of IGM enrichment have successfully explained this as the result of a decreasing fraction of carbon in the triply-ionized state, offsetting the concurrent rise in total carbon density (Oppenheimer & Davé 2006; Davé & Oppenheimer 2007; Oppenheimer & Davé 2008).

Models of enrichment and carbon ionization at $z > 4$ have been able to produce a rise in $\Omega_{\text{C IV}}$ between $z = 6$ and 5 consistent with the observations (Oppenheimer, Davé & Finlator 2009; Cen & Chisari 2010), at least within their large uncertainties. Both Oppenheimer et al. (2009) and Cen & Chisari (2010) find that the total amount of carbon in the IGM increases by a factor of 2.5 to 3 in this interval, while the fraction of carbon in the triply-ionized state only increases by a factor of $\lesssim 1.25$.

These simulations do not self-consistently model reionization, so they are unable to directly elucidate the relationship between reionization and enrichment, and therefore unable to provide a satisfying solution to the first puzzle posed above, which is our primary concern here. We are therefore interested in investigating the connections between reionization, enrichment, and the population of galaxies responsible for both.

3 METHODS

3.1 Connecting Reionization and the Galaxy Luminosity Function

In order to solve the two puzzles posed by the rapid $\Omega_{\text{C IV}}$ rise between $z = 6$ and 5 (§1), we need to model the luminosity function of galaxies, and from that model calculate the total ionizing emissivity as a function of redshift. We assume the LF is a Schechter function. Observations suggest that ϕ_* (the density normalisation) and α (the faint-end slope of the LF) are approximately constant from $z = 4$ to 6 (Bouwens et al. 2007). Neither are constrained as precisely at higher redshift, but Bouwens et al. (2010) find that the observed LF at $z = 7$ and 8 is consistent with constant α and ϕ_* , though the maximum-likelihood values move toward steeper faint-end slopes ($\alpha = -1.94 \pm 0.24$ at $z \sim 7$ and -2.00 ± 0.33 at $z \sim 8$). We therefore parameterise the evolution of the LF by varying only M_* with redshift. At $z < 9.0$ we use the M_* values from Bouwens et al. (2008), linearly interpolated as a function of redshift. At $z > 9$ we assume M_* is linear in redshift with slope β_{M_*} . The parameters α and β_{M_*} therefore control the extrapolation of the

LF to lower luminosities and higher redshifts than have yet been probed by observations.

To convert the observed LF to an ionizing photon emissivity (or rate density, photons⁻¹ s⁻¹ Mpc³), we use the Bolton & Haehnelt (2007) spectral energy distribution (SED) and an escape fraction $f_{\text{esc}\gamma}$. With this SED, the ratio of ionizing photon production rate to UV luminosity is

$$\frac{\dot{N}}{L(1500 \text{ \AA})} = 8.4 \times 10^{24} \frac{\text{photons s}^{-1}}{\text{erg s}^{-1} \text{ Hz}^{-1}}, \quad (3)$$

though we assume only a fraction $f_{\text{esc}\gamma}$ of these escape into the IGM.³

With these factors we convert the integrated LF history into an ionizing emissivity history, and then into the ionized fraction of the IGM $x(z)$. We ignore twice-ionized helium, assume that once-ionized helium has the same number fraction as hydrogen, and include recombinations of hydrogen. Recombinations are calculated with clumping factor $C \equiv \langle n_{\text{HII}}^2 \rangle / \langle n_{\text{HII}} \rangle^2 = 4$ (see §4.1 for discussion of varying C), gas temperature 10^4 K (giving case B recombination rate $\alpha_B = 2.6 \times 10^{-13} \text{ cm}^3 \text{ s}^{-1}$, Hui & Gnedin 1997) and assuming all ionized gas is contained in fully ionized bubbles. We integrate the LF down to $M_{\text{AB}}(\text{UV}) = -13.04$, equivalent to a star formation rate of $0.01 m_{\odot}/\text{yr}$ (Kennicutt 1998; Oesch et al. 2009). We use the ‘‘WMAP7 + BAO + H0’’ mean cosmological parameters from Komatsu et al. (2010) throughout this paper. The values of $f_{\text{esc}\gamma}$, β_{M_*} , and α are discussed in §4.

3.2 Connecting Reionization and Carbon Production

We define $f_{x\text{CIV}}$ as the ratio between the total rate (with no delay) of CIV production and the total rate of ionizing photon production, so that:

$$\dot{\Omega}_{\text{CIVinst}}(z) = \dot{x}_{\text{total}}(z) f_{x\text{CIV}}, \quad (4)$$

where $\dot{\Omega}_{\text{CIVinst}}(z)$ would be the rate of CIV density increase with no delay in emission, and $\dot{x}_{\text{total}}(z)$ is the ratio of the total rate density of ionizing photon production to the total number density of hydrogen and helium atoms.

The $f_{x\text{CIV}}$ ratio depends on a number of factors:

$$f_{x\text{CIV}} = \left[\frac{f_{\text{CIV}} f_{\text{esc}Z}}{r_{\gamma Z}} \right] (X_C/Z) \Omega_{\text{baryon}}. \quad (5)$$

The fraction of all metal mass in carbon is $X_C/Z = 0.178$ (the solar value from Asplund, Grevesse & Sauval 2005). $\Omega_{\text{baryon}} = 0.0456$ is the fraction of the critical density contributed by baryons (Komatsu et al. 2010). The terms in square brackets (the fraction of carbon in CIV, f_{CIV} ; the fraction of metals that escape galaxies, $f_{\text{esc}Z}$; and the ratio of metal nucleon to ionizing photon production, $r_{\gamma Z}$) are highly uncertain. We use the representative values of $f_{\text{CIV}} = 0.5$ (the maximum theoretical value, see Ryan-Weber et al. 2009; Songaila 2001) and $f_{\text{esc}Z} = 0.2$ (equal to our fiducial

$f_{\text{esc}\gamma}$), and emphasise that it is only the product of these uncertain factors that matters.

The ratio of ionizing photons to metal nucleons produced by a stellar population can be expressed as

$$r_{\gamma Z} = \eta \frac{E_p}{E_{\text{avg}}}, \quad (6)$$

where η is the ratio of total ionizing photon energy to total rest-mass energy of the metals produced in a stellar population, E_p is the rest-mass energy of a proton, and E_{avg} is mean energy of ionizing photons (Schaerer 2002). For a stellar population with $Z = 1/50 Z_{\odot}$, Schaerer (2002) calculate $\eta = 0.014$ and $E_{\text{avg}} = 21.95$ eV, yielding $f_{x\text{CIV}} = 1.4 \times 10^{-9}$. Note that this η value does not include yields from low- and intermediate-mass stars (LIMS, $m < 8m_{\odot}$), stellar wind mass loss, or Type I SN contributions, all of which would decrease η (and increase the enrichment to ionization ratio $f_{x\text{CIV}}$). We will also explore scenarios using the solar-metallicity ($Z = Z_{\odot}$) values of $\eta = 0.0036$ and $E_{\text{avg}} = 20.84$ eV (calculated with mass loss and SN Ibc, but still without LIMS), resulting in $f_{x\text{CIV}} = 5.0 \times 10^{-9}$.

Changing the M_* vs. z slope (β_{M_*}) or the faint-end slope of the LF (α) changes both the ionization and enrichment histories. Changing $f_{\text{esc}\gamma}$ only affects the ionization history. Changing $f_{x\text{CIV}}$ only affects the enrichment history.

3.3 The Carbon Delay Distribution Due to Stellar Lifetimes

Carbon is not produced instantly upon formation of a population of stars, unlike, for our purposes, ionizing photons. Instead carbon is ejected primarily after the main-sequence lifetime of a star is over, which for low and intermediate mass stars ($m \lesssim 8m_{\odot}$, $t_{\text{life}} \gtrsim 3 \times 10^7$ years) becomes a significant fraction of the relevant timescales (e.g. the 3×10^8 year interval from $z = 6$ to 5).

Neglecting this delay (as in Cen & Chisari 2010) is often justified with the statement that Type II supernova (SNII) yields from short-lived, high-mass stars dominate carbon production at high redshift. However, even if most carbon is synthesised in SNeII⁴, a substantial fraction of that carbon is incorporated into low- and intermediate-mass stars (LIMS, $m \lesssim 8m_{\odot}$) before being blown into the IGM, according to the models of Oppenheimer & Davé (2008). In other words, an important fraction of carbon produced in a galaxy gets locked up in LIMS and is only returned to the gas phase (and made available for ejection in a galactic outflow) during the asymptotic giant branch (AGB) phase, after the main-sequence lifetime has elapsed. Therefore, the lifetimes of lower-mass stars impose a delay on the ejection of some of the carbon into the IGM, and AGB star ejection of carbon cannot be neglected in calculating the timing of IGM enrichment.

⁴ The fraction of carbon contributed by low and intermediate mass stars depends sensitively on the amount of ‘‘hot bottom burning’’ (HBB) that takes place on the asymptotic giant branch (AGB), since HBB can destroy carbon and even result in a net loss of ¹²C over the lifetime of a star. The amount of HBB as a function of stellar mass is still highly uncertain, (Ventura & Marigo 2010) so it is unclear whether low- or high-mass stars dominate ¹²C production (Romano et al. 2010, and references therein).

³ Note that $\dot{N}/L(1500 \text{ \AA})$ is sensitive to the initial mass function and metallicity of the stellar population, though we ignore this dependence here. $\dot{N}/L(1500 \text{ \AA})$ is completely degenerate with $f_{\text{esc}\gamma}$ in our formalism.

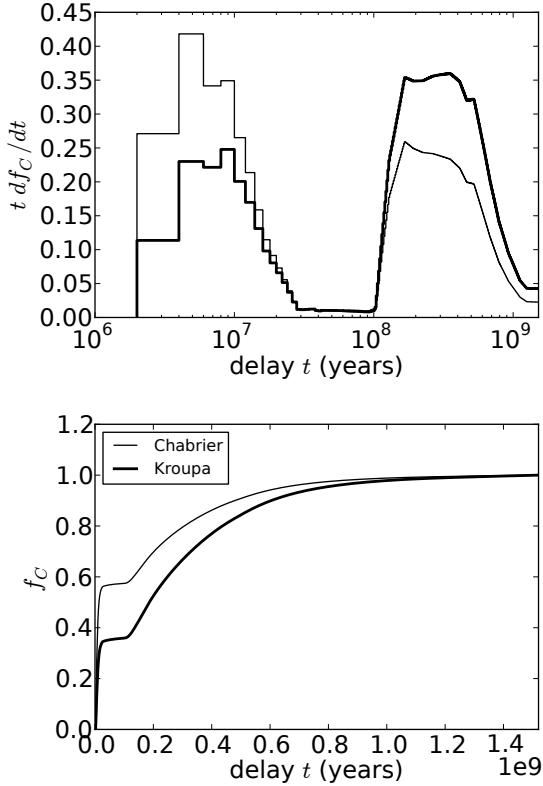


Figure 1. Delay functions for carbon production. Differential (top panel) and cumulative (bottom panel), delays are calculated with Chabrier (thin curve) and Kroupa (thick curve) IMFs. The differential delay is shown on a logarithmic time scale, while the cumulative delay is shown on a linear time scale. Note the rapid emission from supernovae ($\sim 10^7$ years) and the longer tail from AGB stars (\sim a few $\times 10^8$ years).

Since we are trying to model the connection between ionizing emission associated with star formation and the eventual enrichment of the IGM with carbon produced by the same stars, it is important that we take this delay into account. Indeed, such a delay is inevitable, and the original motivation of this paper was to assess whether this delay might help explain the steep observed evolution of the C IV abundance in the IGM, as discussed in §1.

The cumulative delay function $f_C(t)$ is the fraction of carbon emitted by stars with lifetimes $t_{\text{life}} < t$. Assuming all carbon is ejected at the end of a star’s main sequence lifetime, the fraction of carbon ejected in the time interval $t \pm (dt/2)$ after star formation is

$$\frac{df_C}{dt}(t) = \frac{df_C}{dm} \frac{dm}{dt}, \quad (7)$$

where dm/dt is the inverse of the derivative of the lifetime function ($t_{\text{life}}(m)$). The fraction of carbon produced by stars of mass $m \pm (dm/2)$ is

$$\frac{df_C}{dm}(m) \propto M_C(m)\phi(m), \quad (8)$$

where $M_C(m)$ is the carbon mass ejected by a star of mass m , and $\phi(m)$ is the initial mass function (IMF) of stars by

number. We normalise this function to give $\int_{t_{\text{min}}}^{t_{\text{max}}} df_C/dt = 1$. Here $t_{\text{min}} = 3.24 \times 10^6$ years is the lifetime of a $100M_{\odot}$ star, and $t_{\text{max}} = 1.52 \times 10^9$ years is the cosmic time between the starting and ending points of our simulations, $z = 100$ and $z = 4.1$. With our chosen IMFs and yields (see below), an additional $< 9\%$ of carbon would emerge at $t > t_{\text{max}}$.

Convolving the $\Omega_{\text{C IV inst}}(t)$ curve with $\frac{df_C}{dt}$ gives us the delayed C IV curve

$$\Omega_{\text{C IV delay}}(t) = \Omega_{\text{C IV inst}} * \left(\frac{df_C}{dt} \right), \quad (9)$$

where $*$ represents convolution over the time coordinate.

Romano et al. (2005, 2010) have quantified in detail the impact of uncertainties in the IMF, stellar lifetimes, and stellar yields on Galactic chemical evolution models. The greatest uncertainties are in the yield calculations, which vary considerably from author to author. As Romano et al. (2010) point out, there is no consistent set of yields covering the whole range of mass and metallicity and including all of the physical effects relevant to either galactic or cosmic chemical evolution models, and essentially no suitable calculations have been performed for $m \approx 6 - 8M_{\odot}$. For convenience, we use a set of carbon (^{12}C) yield values provided by Gavilán, Buell & Mollá (2005)⁵, containing their own original calculations for $m = 1-8M_{\odot}$, and Woosley & Weaver (1995) values for $m = 8 - 100M_{\odot}$. We use the yields for metallicity $Z = 0.02$ because the variation in calculated carbon yield with metallicity (at least above some threshold) is smaller than the overall uncertainty in yields.

The final complication with the use of yield tables is the distinction between the total mass of an element ejected by a star and the net yield of new atoms synthesised in the star (Gavilán et al. 2005). In a self-consistent chemical evolution model that tracks the metallicity of the star-forming environment, the yield of new elements is the relevant quantity. However, we are only tracking carbon abundance in the IGM, while stars are forming directly out of gas in the interstellar medium (ISM), so we use the total ejected mass of carbon to calculate the delay. Note that this is independent of the calculation of the total amount of carbon produced (see §3.2). This is a good approximation if the ISM reaches a stable metallicity quickly, and the composition of the galactic outflow is representative of the total mass currently being ejected from stars (both via SN and AGB mass loss).

Theoretical calculations of stellar lifetimes generally agree fairly well for $m > 1M_{\odot}$. The dependence on metallicity is quite weak. The larger uncertainties at $m < 1M_{\odot}$ are irrelevant here since the corresponding lifetime of $t_{\text{life}} > 10$ Gyr is longer than the age of the universe at $z > 0.3$. We adopt the lifetime function of Kodama as given in Romano et al. (2005).

The stellar initial mass function is another important source of uncertainty. We can characterise the impact of the IMF on the delay function by dividing the carbon emission into a prompt component and a delayed component. We are concerned here with evolution on a timescale of $\sim 10^8$ years. Therefore carbon emission that occurs faster than 10^7 years after star formation is relatively prompt. Of the IMFs discussed in the Romano et al. (2005) review, the

⁵ Available on VizieR: <http://vizier.u-strasbg.fr>

Kroupa, Tout & Gilmore (1993) and Chabrier (2003) IMFs produce the most extreme values for the cumulative delay function at 10^7 years, $f_C(10^7\text{yr})$. With a Kroupa IMF $f_C(10^7\text{yr}) = 0.23$, while $f_C(10^7\text{yr}) = 0.44$ for a Chabrier IMF. We therefore calculate all of our models with both of these IMFs⁶ in order to demonstrate quantitatively the impact of the IMF uncertainty on our results, and to suggest qualitatively the impact that different sets of yield values might have. Figure 1 shows the differential and cumulative delay functions with Kroupa and Chabrier IMFs. These figures illustrate that roughly half of the carbon ejection occurs essentially instantly, whereas the remaining half is spread over the lifetime ($\sim 1\text{Gyr}$) of intermediate-mass stars.

Extremely low metallicities may result in dramatically different IMFs and yields from those assumed here. We do not consider this metal-free, or Population-III, mode of star formation in calculating the delay function, as metal-free stars are thought to make up only a small fraction of the stars formed before $z = 6$, even if their formation continues at a low rates to late times (see, e.g. Rollinde et al. 2009; Salvaterra et al. 2010).

4 RESULTS

The primary constraints on the epoch of reionization available today are the *WMAP* measurement of τ (the optical depth to Thomson scattering from free electrons in the IGM, Komatsu et al. 2010) and the evolving Lyman- α opacity of the IGM at $z \sim 6$ (though see Mesinger 2010 for a discussion of the complicated, model-dependent interpretation of this evolution). In §4.1, we discuss the agreement between our luminosity function histories and these reionization constraints. Then in sections 4.2 and 4.3, using the formalism outlined above, we return to the puzzles posed in the introduction.

4.1 Matching Reionization Constraints

In this section, we compare our luminosity function histories to available constraints on the reionization of the IGM. For our fiducial luminosity function history, we adopt a Schechter luminosity function with fixed $\phi_* = 1.1 \times 10^{-3} \text{ Mpc}^{-3}$ and α , and use the observed M_* values from Bouwens et al. (2008) (linearly interpolated) from $z = 3.8$ to 9.0. We extrapolated M_* linearly in z above $z = 9$ with slope β_{M_*} . The extrapolation to lower luminosities is controlled by the faint-end slope, α . Oesch et al. (2009) suggest that M_* is approximately linear in z at high redshift, with a slope of $\beta_{M_*} = 0.36 \pm 0.18$. Bouwens et al. (2008) suggest $\alpha = -1.74$ at high redshift. We use $f_{\text{esc}\gamma} = 0.2$.

Figure 2 shows the ionization and enrichment histories as functions of redshift. The lower (blue) set of curves corresponds to the fiducial parameters described above. The top panel shows the ionized fraction in the IGM, along with the optical depth integrated from redshift 0 to z . The arrows

⁶ Note that we are only varying the IMF in the calculation of the delay function. In principal $\dot{N}/L(1500 \text{ \AA})$ and $r_{\gamma Z}$ also depend on the IMF and metallicity of the stellar population, but we treat each of these calculations independently.

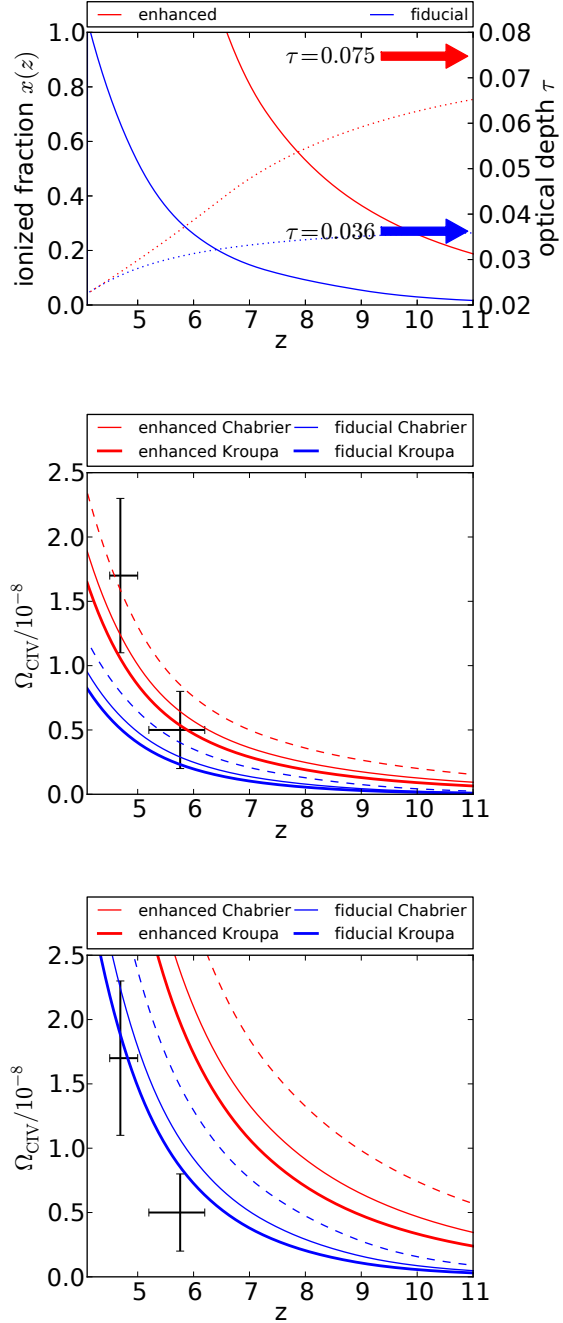


Figure 2. Ionization and enrichment histories of the IGM. In each panel, the lower (blue) set of curves corresponds to the fiducial LF history, and the upper (red) set to the enhanced LF chosen to match *WMAP* $\tau = 0.087$ and $z_{\text{reion}} \sim 6.6$. Top panel: ionized fraction $x(z)$ (solid) and optical depth $\tau(<z)$ (dotted). The arrows on the right show the total value of the optical depth (integrated to $z = 100$). Middle panel: C IV density in the IGM with (solid) and without (dashed) a delay function. The thin solid curve uses the Chabrier-IMF delay, while the thick curve uses the Kroupa-IMF delay. Observed values are indicated as black data points with error bars. Horizontal error bars indicate the interval over which the density is averaged, and vertical error bars indicate the uncertainty. Bottom panel: Enrichment in the same models as in the middle panel, except with $f_{x\text{CIV}}$ increased by a factor of 3.7. This increase is equivalent to the difference between 1/50-solar and solar-metallicity values for the ratio of ionizing photons to metal nucleons.

on the right show the total value of the optical depth (integrated to $z = 100$). As Oesch et al. (2009) have pointed out (see also Bolton & Haehnelt 2007), combining this luminosity function evolution with reasonable ionizing photon escape fraction ($f_{\text{esc}\gamma} = 0.2$) and IGM clumping factor ($C = 4$) values, yields an insufficient emissivity to either complete reionization by $z \sim 6$ or match the *WMAP* constraint on the electron scattering optical depth ($\tau = 0.087 \pm 0.014$ Komatsu et al. 2010). With the fiducial LF history, the IGM is only 20% ionized by $z = 6$, and the optical depth is $\tau = 0.036$.

In order to match the *WMAP* τ value and complete reionization at $z \gtrsim 6$, we increase $f_{\text{esc}\gamma} \dot{N}/L(1500 \text{ \AA})$ by a factor of 3, flatten the M_* slope to $\beta_{M_*} = 0.09$, and set the faint end slope to the steeper value of $\alpha = -1.95$. The higher $f_{\text{esc}\gamma} \dot{N}/L(1500 \text{ \AA})$ could be explained by a higher escape fraction, or a higher $\dot{N}/L(1500 \text{ \AA})$ due to a lower metallicity or more top-heavy IMF of the stellar population. For instance, Chary (2008) finds a factor of ~ 2 – 3 increase in $\dot{N}/L(1500 \text{ \AA})$ when the metallicity falls from $0.4Z_{\odot}$ to $0.02Z_{\odot}$. Note that such changes would affect the delay function and $r_{\gamma Z}$ values as well. The changes to β_{M_*} and α make the enhanced LF history resemble the recent results by Bouwens et al. (2010), who found a brighter M_* and steeper α at $z = 7$ and 8 than were suggested by earlier results. We integrate the LF down to $M_{\text{AB}}(UV) = -13.04$, equivalent to a star formation rate of $0.01 m_{\odot}/\text{yr}$ (Kennicutt 1998; Oesch et al. 2009). Adjusting any of these parameters alone cannot match both constraints, and adjusting them simultaneously allows us to use more plausible values. More important than the exact parameter values is the resulting ionizing emissivity history. This is obviously not a unique solution, but we present this enhanced LF history as a plausible example of one that matches current observational constraints much better than the fiducial extrapolation of the observed LBG luminosity function. The upper (red) sets of curves in Figure 2 correspond to this enhanced LF history. The top panel shows that the optical depth has been increased to near the *WMAP* value, and the IGM is fully ionized by $z = 6.6$. Table 1 summarises the parameters of each LF history.

We use a constant clumping factor $C = 4$ in these calculations, though our basic conclusion that the enhanced LF history is consistent with existing reionization constraints is not particularly sensitive to changes in this assumption. For instance, using a higher constant $C = 6$ results in $\tau = 0.067$, $z_{\text{reion}} = 6.21$ for the enhanced LF history. The clumping factor should actually be lower at higher redshift, however. Chary (2008) has derived the clumping factor as a function of redshift for the relevant gas (ionized gas outside of ionizing-photon source halos) from simulations by Trac & Cen (2007). Using their clumping factor history (estimated from their Figure 2a), results in a larger $\tau = 0.082$ (because the clumping factor is lower, $C < 4$, at early times, $z > 10.5$) and a later $z_{\text{reion}} = 5.7$ (because $C \gtrsim 8$ at $z \lesssim 7$). This optical depth is quite close to the *WMAP* value. Pawlik, Schaye & van Scherpenzeel (2009a,b) found that reheating of the IGM results in an even lower clumping factor history, which would require less enhancement in the LF history (something between our “fiducial” and “enhanced” LFs) to match reionization constraints.

Table 1. Parameters of our luminosity function (LF) histories.

name	α	β_{M_*}	$f_{\text{esc}\gamma}$	z_{reion}	τ
fiducial	-1.74	0.36	0.2	4.2	0.036
enhanced	-1.95	0.09	0.6	6.6	0.075
<i>WMAP7</i> (Komatsu et al. 2010):					0.087 ± 0.014

Parameters:

α is the faint-end slope of the Schechter luminosity function.

β_{M_*} is the slope of M_* as a function of z .

$f_{\text{esc}\gamma}$ is the escape fraction of ionizing photons from galaxies. Note that it is completely degenerate with the SED slope, which we fix at $\dot{N}/L(1500 \text{ \AA}) = 8.4 \times 10^{24} \text{ photons s}^{-1}/(\text{erg s}^{-1} \text{ Hz}^{-1})$.

Results:

z_{reion} is the redshift at which the ionized fraction $x(z) = 1$.

τ is the optical depth due to free electrons.

4.2 Matching CIV Abundance

The bottom two panels of Figure 2 display the CIV mass density as a fraction of the critical density $\Omega_{\text{CIV}}(z)$. The dashed lines assume instantaneous ejection, the thin solid lines are convolved with the Chabrier-IMF-based delay function, and the thick solid lines with the longer Kroupa-IMF delay.

In order to show the effect of the large uncertainty in the value of $f_{x\text{CIV}}$, in the middle panel we use the $1/50 Z_{\odot}$ value for $f_{x\text{CIV}}$, while in the bottom panel we use the solar-metallicity value (see §3.2). The solar-metallicity stellar population produces fewer ionizing photons per metal nucleon synthesised, so for a fixed LF history it produces higher Ω_{CIV} values. Both of the puzzles discussed in §1 are evident in the middle panel, which effectively uses the same $f_{x\text{CIV}}$ assumed by Ryan-Weber et al. (2009).

First we can see the conflict suggested by Ryan-Weber et al. (2009) between reionization constraints and the low $z = 5.8 \Omega_{\text{CIV}}$ value in the middle panel of Figure 2. The enrichment history calculated from the LF history that matches reionization constraints (upper/red dashed curve) produces too much CIV at $z = 5.8$.⁷ This overproduction at a single redshift, in and of itself, is not too troubling. Either a slight decrease in the highly-uncertain $f_{x\text{CIV}}$ or a slight decrease in the star formation rate density (SFRD) could lower Ω_{CIV} sufficiently to agree with the $z = 5.8$ measurement. Also, the stellar-lifetime delay, especially with the less top-heavy Kroupa IMF, brings Ω_{CIV} down to close to the observed value.

The second puzzle — the rapid buildup of CIV from $z = 5.8$ to 4.7 noted by Becker et al. (2009) — is also evident in Figure 2. In the middle panel, again, the enhanced LF curve with no delay is close to matching the $z = 4.7$ observation, but slightly over-predicts the earlier $z = 5.8$ point. Similarly, the fiducial LF curve with no delay only slightly under-predicts the $z = 5.8$ value, but is much lower than the later $z = 4.7$ observation. The predicted evolution

⁷ Again, we are ignoring the large errors on the observations for the sake of exploring their consequences should they prove to be accurate. If we take the observational errors into account, then we can see that even the upper/red dashed curve is marginally consistent with the observations.

of Ω_{CIV} using either LF history is too slow to match the observations.

We were motivated to calculate the stellar–lifetime–based enrichment delay by the idea that such a delay might help to explain the rapid rise in C IV. In fact, as Figure 2 clearly illustrates, we find that stellar lifetimes contribute little to the solution of this puzzle. In the next subsection, we explore the effect of longer delays.

4.3 The Rapid Rise in CIV

Since $f_{x\text{CIV}}$ is so uncertain, it is useful to find a quantity independent of $f_{x\text{CIV}}$ to compare with the observations. For a given combination of an ionizing emissivity history and a delay function, the fractional increase in Ω_{CIV} over a specific redshift interval is fixed and does not depend on $f_{x\text{CIV}}$ (as long as $f_{x\text{CIV}}$ is independent of redshift). The observed fractional increase is

$$\frac{\Delta\Omega_{\text{CIV}}}{\Omega_{\text{CIV}}} \equiv \frac{\Omega_{\text{CIV}}(4.7)}{\Omega_{\text{CIV}}(5.8)} - 1 = 2.4. \quad (10)$$

To compare this number with our theoretical curves, we average Ω_{CIV} over the same intervals used to determine the observed values. With no delay, the fractional increase is $\Delta\Omega_{\text{CIV}}/\Omega_{\text{CIV}} = 0.79$ for the fiducial LF history, and 0.70 for the enhanced LF history. These values are far smaller than the observed increase.

We expect a delay in enrichment to make the fractional increase in C IV larger, because (if Ω_{CIV} evolves slower than exponentially) the fractional rate of increase at earlier times must be higher. To see this, consider that the fractional increase is roughly

$$\frac{\Delta\Omega_{\text{CIV}}}{\Omega_{\text{CIV}}} \approx \frac{\dot{\Omega}_{\text{CIV}}}{\Omega_{\text{CIV}}}(t)\Delta t, \quad (11)$$

where $\Delta t \sim 0.3$ Gyr is the time interval from $z = 5.8$ –4.7 and $\dot{\Omega}_{\text{CIV}}$ is the derivative of Ω_{CIV} with respect to cosmic time. If Ω_{CIV} is a power–law, proportional to t^n (this is a reasonable approximation at the cosmic times we are considering, and it is also a conservative one, in the sense that structure formation is increasingly more rapid at higher redshifts), then

$$\frac{\dot{\Omega}_{\text{CIV}}}{\Omega_{\text{CIV}}}(t) = \frac{n}{t}. \quad (12)$$

Therefore, the fractional growth rate decreases with time. If we had a delta–function delay, so that $\Omega_{\text{CIVdelay}}(t) = \Omega_{\text{CIVinst}}(t - t_{\text{delay}})$, then the delay would boost the fractional increase by a factor of

$$\frac{\dot{\Omega}_{\text{CIVdelay}}/\Omega_{\text{CIVdelay}}}{\dot{\Omega}_{\text{CIVinst}}/\Omega_{\text{CIVinst}}} \sim \frac{t}{t - t_{\text{delay}}}. \quad (13)$$

We need a factor of $t/(t - t_{\text{delay}}) = 3$ –3.5 to boost the fractional C IV increase from $\Delta\Omega_{\text{CIV}}/\Omega_{\text{CIV}} = 0.7$ –0.8 to 2.4. We can conclude that a delta–function delay of ~ 0.7 Gyr should boost the growth sufficiently to match the slope inferred from the two observations. Our stellar–lifetime–based delays, however, are too short to provide the necessary boost. The mean delay with the Chabrier IMF is 0.16 Gyr. With the Kroupa IMF, the mean delay is only slightly longer, 0.25 Gyr. Furthermore, and even more problematically, the delay is not a delta function. A large fraction (roughly half; see

Table 2. Fractional increase in C IV density for each luminosity function history and delay function combination.

LF History	Delay Function (1)	$f_{x\text{CIV}}/10^{-9}$ (2)	$\Delta\Omega_{\text{CIV}}/\Omega_{\text{CIV}}$ (3)
<i>observed Ω_{CIV} evolution</i>		—	2.4
enhanced	no delay	1.5	0.7
enhanced	Chabrier	1.9	0.7
enhanced	Kroupa	2.3	0.8
enhanced	0.5 Gyr delta	4.5	1.1
enhanced	Cha + 0.5 Gyr	6.2	1.3
enhanced	Krp + 0.5 Gyr	7.8	1.5
enhanced	0.6 Gyr delta	5.9	1.4
enhanced	Cha + 0.6 Gyr	8.4	1.8
enhanced	Krp + 0.6 Gyr	10.7	2.1
enhanced	0.7 Gyr delta	7.9	2.1
enhanced	Cha + 0.7 Gyr	11.8	2.6
enhanced	Krp + 0.7 Gyr	15.7	3.1
fiducial	no delay	3.0	0.8
fiducial	Chabrier	3.9	0.9
fiducial	Kroupa	4.7	1.0
fiducial	0.5 Gyr delta	10.8	2.3
fiducial	Cha + 0.5 Gyr	16.3	2.7
fiducial	Krp + 0.5 Gyr	21.7	3.2
fiducial	0.6 Gyr delta	15.6	4.0
fiducial	Cha + 0.6 Gyr	24.7	4.8
fiducial	Krp + 0.6 Gyr	34.6	5.4
fiducial	0.7 Gyr delta	25.4	8.2
fiducial	Cha + 0.7 Gyr	42.7	9.5
fiducial	Krp + 0.7 Gyr	62.5	10.5

(1) Figure 3 shows the corresponding enrichment history for each row in this table (except the 0.6 Gyr delays).

(2) The $f_{x\text{CIV}}$ value given is the one needed to match Ω_{CIV} at $z = 4.7$. Compare to our estimates of $f_{x\text{CIV}} = 1.4 \times 10^{-9}$ for $Z = 1/50 Z_{\odot}$, or 5.0×10^{-9} for $Z = Z_{\odot}$.

(3) $\Delta\Omega_{\text{CIV}}/\Omega_{\text{CIV}}$ is independent of $f_{x\text{CIV}}$.

Figure 1) of the carbon is ejected promptly, which dilutes the boosting effect.

Figure 3 shows enrichment histories with $f_{x\text{CIV}}$ adjusted to fit $\Omega_{\text{CIV}}(z = 4.7)$ to the observed value. This allows us to assess the effect of the delay on the slope by comparing the earlier evolution of the Ω_{CIV} curve to the observed value at $z = 5.8$. If C IV absorber production is too slow, $\Delta\Omega_{\text{CIV}}/\Omega_{\text{CIV}}$ will be too small, and we will over–predict the earlier measurement. Table 2 gives the $f_{x\text{CIV}}$ and $\Delta\Omega_{\text{CIV}}/\Omega_{\text{CIV}}$ values for each combination of LF history and delay function. In Figure 4, we plot $\Delta\Omega_{\text{CIV}}/\Omega_{\text{CIV}}$ as a function of the delay.

The stellar–lifetime delays alone are insufficient to boost the C IV growth to the observed rate, whereas assuming a 0.7 Gyr delay instead brings the enhanced LF history into agreement with the observations (top panel of Figure 3). Since the stellar–lifetime delay is inevitable, even if a longer delay is also in effect, we next add the 0.7 Gyr delay to the stellar–lifetime–based delay (middle panel of Figure 3). When the stellar–lifetime delays are added, the fractional growth is increased by 25–50% (for the Chabrier and Kroupa delays, respectively). In the bottom panel of Figure 3 we add a shorter 0.5 Gyr delay. Table 2 also includes an intermediate

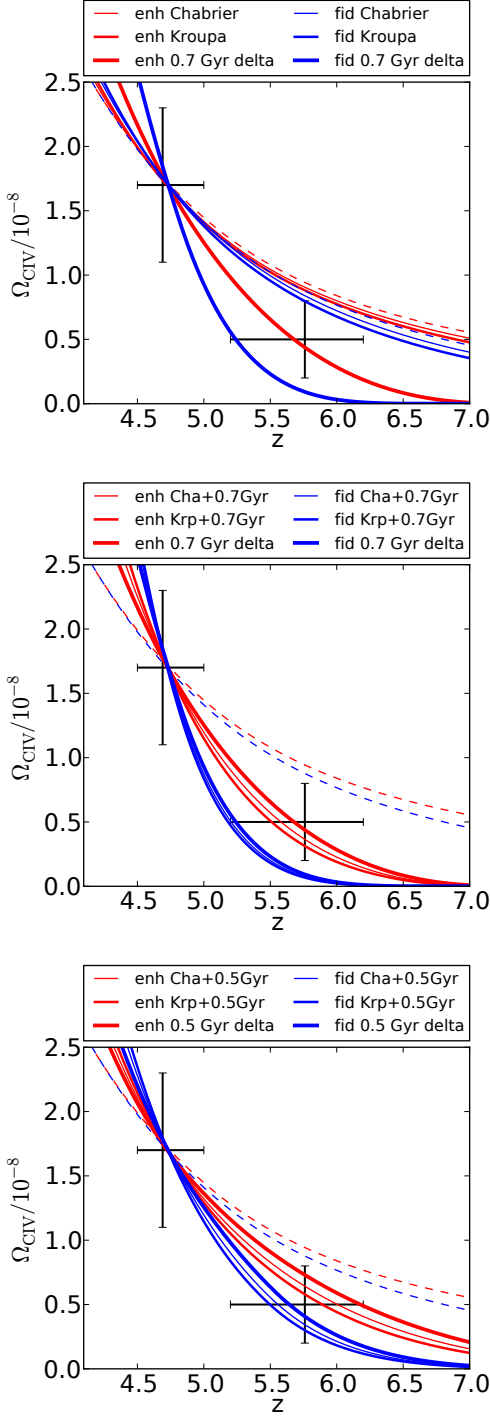


Figure 3. Enrichment histories with the stellar carbon-to-ionizing-photon production ratio, $f_{x\text{CIV}}$, adjusted to match the $z = 4.7$ observation. The dashed curves assume instantaneous production of C IV. Top panel: comparing stellar-lifetime-based delays and a 0.7 Gyr delta function delay. Middle panel: a 0.7 Gyr delay has been added to the stellar-lifetime delays. Bottom panel: a 0.5 Gyr delay has been added to stellar-lifetime delays.

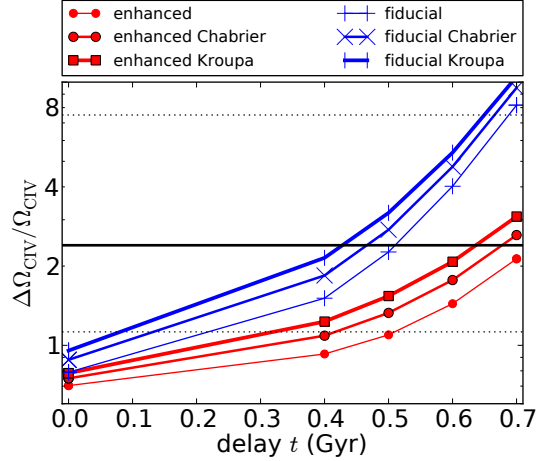


Figure 4. Fractional increase in C IV density as a function of the additional delay t . Note the log scale of the vertical axis. The bottom three curves show the fractional increase in C IV density from $z = 5.8$ to 4.7 for the enhanced luminosity function history with no stellar-lifetime delay, the Chabrier-IMF-based delay, and the Kroupa-IMF-based delay (bottom to top). The top three curves show the corresponding increases with the fiducial LF history. The delay t is *in addition* to any stellar-lifetime delay. The solid horizontal line indicates the observed value of the increase (2.4), while the dotted lines show the (1σ) confidence limits on $\Omega_{\text{CIV}}(z = 5.8)$. The curves with the additional stellar-lifetime delay (top two in each set) match the observed value at $t = 0.4$ to 0.7 Gyr, depending on the LF and IMF.

0.6 Gyr additional delay. Figure 4 allows an easy comparison between the predicted and observed values of $\Delta\Omega_{\text{CIV}}/\Omega_{\text{CIV}}$.

The stellar-lifetime delays have an effect on both the length of the additional delay and the $f_{x\text{CIV}}$ value needed to match the observations. For instance, with the enhanced LF history and a delta function delay of 0.7 Gyr, the fractional increase is 2.1 and $f_{x\text{CIV}} = 7.9 \times 10^{-9}$. With the Kroupa-IMF delay included, a shorter additional delay of 0.6 Gyr produces the same fractional increase, but then $f_{x\text{CIV}}$ must be increased by 35%. Therefore, future models designed to study the relationships between reionization, enrichment, and galaxy formation must include the finite stellar lifetimes in order to draw precise quantitative conclusions.

While some of the $f_{x\text{CIV}}$ values in Table 2 are physically plausible, some may be unphysically high, indicating that certain delay function and LF history combinations are not reasonable candidates for explaining the observed increase in C IV density. For instance, the fiducial LF with a delta-function delay of 0.7 Gyr requires the rather high value of $f_{x\text{CIV}} = 2.5 \times 10^{-8}$. On the other hand, $f_{x\text{CIV}} = 7.9 \times 10^{-9}$ (for the enhanced LF history with 0.7 Gyr delay function delay) could plausibly be explained as the result of a solar-metallicity $r_{\gamma Z}$ (ionizing photon to metal nucleon ratio) and $f_{\text{esc}Z} = 0.3$ (instead of 0.2).

So far in this section, we have ignored the observational uncertainties on Ω_{CIV} . We are less concerned about the error at $z = 4.7$, since Ω_{CIV} is approximately constant at $z \lesssim 4.7$. Therefore in Figure 4, we indicate the range of the fractional increase corresponding to the 1σ confidence interval on Ω_{CIV} at $z = 5.8$ (dotted lines). The current large ob-

servational errors allow a wide range of values for the delay (e.g. 1σ limits of ~ 0.1 – 0.7 Gyr for the fiducial LF), but Figure 4 makes it clear that the current constraints exclude zero delay at more than the 1σ level, and that a combination of tighter constraints on $\Omega_{\text{CIV}}(z = 5.8)$ and the galaxy luminosity function at $z > 6$ has the potential to place interesting constraints on the delay.

In Figure 4, we have shown that, without any change in the C IV ionization correction, a ~ 0.4 – 0.7 Gyr delay between the production of ionizing photons and C IV absorption features can explain the rapid increase in C IV density between $z = 5.8$ and 4.7 . Simulations (Oppenheimer et al. 2009; Cen & Chisari 2010) suggest that the triply-ionized fraction of carbon may increase by a factor of up to 1.25 in this interval, which would help to explain the observed rise, but would leave a factor of $\gtrsim 2.7$ increase ($\Delta\Omega_{\text{C}}/\Omega_{\text{C}} = 1.7$) in the total carbon content of the IGM. Figure 4 tells us that this growth still requires a delay of ~ 0.6 Gyr with the enhanced LF history, or ~ 0.4 Gyr for the fiducial LF. In the next section we will explore possible physical mechanisms for such delays.

5 DISCUSSION

Since stellar lifetimes were too short to provide the required delay, what mechanism could explain a longer ~ 0.4 – 0.7 Gyr timescale? We show in this section that changing the stellar initial mass function is not a viable explanation, but that galactic outflow timescales correspond nicely to the required delay. We then make testable predictions for two different outflow-driven delay scenarios.

5.1 Failed Explanations for the Delay: the IMF

One way to produce a longer mean delay in carbon production would be to change the stellar IMF to increase the proportion of long-lived, low-mass stars.⁸ To produce the long delay times found above requires an IMF that is radically bottom-heavy at high redshift. Even with a steep power-law IMF of $\phi(m) \propto m^{-3.5}$, we find $\Delta\Omega_{\text{CIV}}/\Omega_{\text{CIV}} < 1.1$. Therefore we also explored using a truncated Salpeter IMF ($\phi(m) \propto m^{-2.35}$) with different maximum masses, and found that a maximum stellar mass of $2.44 m_{\odot}$ (with the fiducial LF) or $2.09 m_{\odot}$ (with the enhanced LF) is required to produce a $\Delta\Omega_{\text{CIV}}/\Omega_{\text{CIV}}$ of 2.4. These stellar masses correspond to lifetimes of 0.4 and 0.6 Gyr, respectively, in agreement with the delay times that we found above. However, these IMFs would produce no ionizing radiation to accomplish reionization, and would not match the constraints on the SEDs of high redshift galaxies. Furthermore, a bottom-heavy IMF is in opposition to the trend expected for stars forming from metal-poor gas (but see Omukai, Schneider & Haiman 2008, who propose that when the metallicity exceeds a critical value of $\sim 10^{-5} Z_{\odot}$, dense

⁸ Though this is outside the stellar mass range we are concerned with, van Dokkum & Conroy 2010 have found evidence for $\phi(m) \propto m^{-3}$ at $m \lesssim 1 m_{\odot}$ in massive local early-type galaxies.

clusters of low-mass stars may form in the nuclei of second-generation galaxies). Therefore changes to the IMF seem totally unable to explain the rapid Ω_{CIV} evolution.

5.2 Explanations for the Delay: Galactic Outflows

In order to explain a long delay between star formation and C IV absorber production, we may posit that carbon ejected from a galaxy must reach a characteristic distance before producing a C IV absorption feature visible in current data sets. In this case, the relevant timescale for a distance d and velocity v would be

$$t = 0.5 \text{ Gyr} \frac{d}{100 \text{ kpc}} \frac{200 \text{ km s}^{-1}}{v}. \quad (14)$$

The characteristic distance from the source galaxy at which C IV is observed can be affected both by the ionization state of the carbon as a function of distance, and the filling factor of observable C IV absorbers. If the volume filling factor of the absorbers is too low, absorption systems will become too rare for detection in the limited set of sight lines currently available.

While the exact relationship between galaxies and absorbers is still highly uncertain (and contested), observations at $z = 2$ – 3 seem consistent with this outflow scenario. Steidel et al. (2010) studied absorption associated with Lyman-break galaxies, both along the line of sight to the galaxies and along the line of sight to background galaxies at impact parameters from 3–125 kpc. They found that the absorber equivalent width in their composite spectra declines slowly with impact parameter ($W_0(\text{CIV}) \propto b^{-0.2}$) up to $b \sim 80$ kpc, after which it quickly drops below their detection limit ($W_0 \sim 0.1 \text{ \AA}$). The absorbers detected by Ryan-Weber et al. (2009) at $z = 5.8$ range from $W_0 = 0.06$ to $\sim 0.7 \text{ \AA}$, which would place them at impact parameters from $b > 60$ to $b > 100$ kpc. They fit the W_0 versus b profile with a model of a spherically-symmetric outflow with a covering fraction by absorbing clouds of $f_{\text{cov}}(r) \propto r^{-0.23}$. The slow decline in covering fraction with distance indicates that the absorbing clouds must be expanding as they move away from the source galaxy (otherwise the covering fraction would go like r^{-2}). For a constant expansion velocity and conserved cloud number $R_C \propto r^{1-\gamma/2}$ when $f_{\text{cov}} \propto r^{-\gamma}$. The inferred cloud radius therefore increases as $R_C \propto r^{0.9}$. The fact that the C IV equivalent width declines more slowly than other ions (for which $f_{\text{cov}} \propto r^{-0.6}$) may indicate that ionization effects are also serving to increase the C IV/C ratio with distance from the source galaxy. Therefore, these observations suggest that both an increasing filling factor of absorbers and an increasing triply-ionized fraction of carbon with distance from the source galaxy could delay the appearance of C IV absorption in the IGM.

Steidel et al. (2010) also use their direct line of sight (impact parameter $b = 0$) absorption profiles to constrain models of the outflow velocity. They reproduce the observed profiles with an accelerating velocity profile (higher velocities farther from the source galaxy) reaching maximum velocities of $\sim 800 \text{ km s}^{-1}$. Given the ~ 100 kpc distance corresponding to absorbers with the equivalent width of the Ryan-Weber et al. (2009) sample, this gives a time scale of $\gtrsim 0.1$ Gyr. With the higher sensitivity of quasar spectra (but using the absorber-absorber correlation function rather than

direct detection of the associated galaxies), Martin et al. (2010) find a larger size for absorption regions of ~ 150 kpc, though they also suggest that the size may be constant in comoving coordinates, which brings the physical size back down to 85–100 kpc at $z = 6$ –5.

Martin et al. (2010) and Tytler et al. (2009), using the distortion between the line-of-sight (redshift space) and transverse correlation functions of quasar spectrum absorbers constrain the peculiar velocity of the average absorber to $\lesssim 200$ km s $^{-1}$. However, these analyses compared the mean or central velocities of the absorbers. Steidel et al. (2010) showed that the absorption profiles are quite precisely centred on the redshift of the source galaxy (at least at low impact parameters and averaged over the angular size of the background galaxy), with the *width* of the profile extending to high velocities. Therefore these results would constrain only the peculiar velocities of the host galaxies, not the outflow velocities.

Both Songaila (2006) and Fox et al. (2007) measured the velocity widths of C IV absorbers, and found them to be correlated with absorber column density. In the former sample, absorbers with column densities comparable to the $z = 5.8$ sample have widths (at one-tenth maximum), of 20–300 km s $^{-1}$, while in the later (a study of DLA- and sub-DLA-associated absorption), all of the absorbers with $\log N(\text{CIV}) \gtrsim 13.6$ have widths of > 100 km s $^{-1}$, and most are 200 km s $^{-1}$ –400 km s $^{-1}$.

Numerical hydrodynamic simulations also seem to suggest that both ionization and filling-factor effects are at work. Oppenheimer et al. (2009) find that C IV absorbers at $z = 6$ tend to have left their source galaxy 0.1–0.5 Gyr earlier, and lie within 10–50 kpc of a galaxy in their simulation (giving average speeds of ~ 30 –300 km/s). They suggest that the ionizing radiation from the source galaxy largely determines the distance at which carbon is seen as C IV. Cen & Chisari (2010) found absorbers at similar distances (~ 70 kpc). In their simulations, collisional ionization is important to the C IV ionization balance, and they suggest that at least some C IV absorbers are produced in shocks formed in galactic outflows.

Oppenheimer et al. (2009) also find that, as metals travel farther from the source galaxy, they enrich less dense regions of the IGM and produce weaker C IV absorption systems. Therefore (neglecting the ionization effects for the moment) absorbers near a galaxy will have a higher column density, but a smaller filling factor (and will therefore be detected more rarely), while absorbers farther from the galaxy will have a lower column densities, but larger filling factors.

Whatever is determining the distance scale, a ~ 0.4 –0.7 Gyr delay could naturally be explained as the result of ~ 200 km/s outflows carrying carbon to distances of ~ 80 –140 kpc before it is seen in C IV absorption.

5.3 Predictions

We have shown that a delay between the production of ionizing photons and of (currently-) detectable C IV absorbers in the IGM can solve the puzzles posed by the rapid rise in Ω_{CIV} between $z \approx 6$ and 5, and have suggested that the delay could be due to either (or to a combination) of two mechanisms associated with galactic outflows. Each mechanism leads to distinct observable predictions.

If the filling-factor evolution dominates the delay, it leads to an interesting prediction: if the C IV has indeed already been ejected from galaxies, and the reason it is not yet seen at the highest redshifts is that it has not yet spread to occupy a detectable filling factor, then future observations, with significantly larger effective lines-of-sight, should uncover much of this hitherto hidden carbon in rare, high-column density C IV absorbers (at low impact parameters to unseen galaxies).⁹ This model would predict that, once the rare, high-column-density end of the column density distribution has been probed, the total integrated Ω_{CIV} curve will be a scaled version of the dashed curves in Figure 3, and the Ω_{CII} curve will be a scaled version of the Ω_{CIV} curve. Together, these observations would confirm that the amount of C IV present in the IGM tracks the cosmic star-formation history, but the rise in the filling factor of C IV systems is driven on a longer timescale, determined by the finite (relatively low) speed of the carbon-transporting winds or outflows. The evolution of the C IV column-density distribution and correlation function will provide constraints on outflow and enrichment models.

On the other hand if ionization effects (either local or universal) determine the delay, then ongoing and future measurements of the density of C II should reveal that much of the missing carbon is hidden in that ionization state. Similarly, observations of Si II, Si III, and Si IV absorbers should reveal a changing ionization balance in that element.

These are clear and feasible ways to discriminate observationally between ionization-driven evolution and outflow-filling-factor-driven evolution. In either case, a careful accounting of the total amount of carbon in the IGM (summing over ionization states and the absorber column density distribution) will reveal whether it tracks the cosmic star-formation history. Any departure from a constant proportionality either indicates a problem with measurements of the star-formation history, or a changing efficiency of carbon production, both of which would be of considerable interest.

6 CONCLUSIONS

We have shown that a ~ 0.4 –0.7 Gyr delay between the production of ionizing photons and C IV absorption features can explain the rapid evolution of the C IV density in the IGM between $z = 5.8$ and 4.7. No change in the ratio of carbon to ionizing photon production (the ionizing efficiency) or in the universal ionization correction for C IV is required. This delay has a natural physical explanation, namely the need to transport carbon a certain distance into the IGM before it is seen in C IV absorption. The distance scale would be determined by a combination of the need to enrich a sufficient volume of the IGM to be detectable in a limited number of quasar sight lines, and possible ionization effects that optimise the C IV fraction at a certain distance from the source galaxy. An outflow of 200 km s $^{-1}$ would carry material to a distance of 80–140 kpc on these timescales.

The shorter delay due to finite stellar lifetimes cannot

⁹ The lack of detection of weak C IV absorbers in the Becker et al. (2009) observations is evidence against the alternative hypothesis that the carbon is hidden in systems too weak to detect with most current spectra.

provide the full explanation for the rapid evolution (even with a steep stellar initial mass function), but must be included in future models in order to properly understand the relationships between galaxy formation, reionization, and enrichment of the IGM.

Future measurements of metal abundance in the IGM will provide important constraints on these relationships. Perhaps the most important improvement will come from probing more quasar lines of sight, both to reduce the uncertainty in the density of absorbers in the currently-detected column-density range ($10^{13.5}$ – $10^{14.5}$; Ryan-Weber et al. 2009), and to search for the rare, high-column-density absorbers that we expect to exist close to galaxies. This search does not require extraordinarily high resolution or signal-to-noise ratio (Oppenheimer et al. 2009), just the identification of more high- z quasars and the taking of their near-IR absorption spectra (though probing the weak end of the column-density distribution will require higher quality spectra). The Multi Unit Spectroscopic Explorer (MUSE; Bacon et al. 2006), an integral field unit for the VLT, will be ideal for directly exploring the relationship between galaxies and IGM absorbers because it will be able to simultaneously obtain spectroscopic redshifts for large numbers of galaxies (up to $z \sim 6.6$) near a quasar line of sight, which can then be compared with the redshift distribution of absorbers seen in the quasar spectrum.

Observations of multiple ionization stages of several elements, using the sensitivity and wavelength coverage of new and future near-IR spectrographs like X-shooter, will break the degeneracy of the factors entering into $f_{x\text{CIV}}$, since some factors should be (approximately) independent of element (such as $f_{\text{esc}Z}$ and $r_{\gamma Z}$), while the fraction of carbon in the CIV stage (f_{CIV}) can be constrained from measurements of CII absorption and of the ionization balance in other species (Ryan-Weber et al. 2009). Detailed physical models will be crucial in interpreting these future observations. Such work is already underway (Oppenheimer et al. 2009; Cen & Chisari 2010), but needs to be improved to model both reionization and enrichment self-consistently.

7 ACKNOWLEDGEMENTS

We would like to thank Francesca Matteucci for discussion of stellar chemical yields. ZH acknowledges financial support by the Polányi Program of the Hungarian National Office for Research and Technology (NKTH). RHK is supported by a Zwicky Fellowship at ETH Zurich. PM would like to acknowledge NSF grant AST-0908910. We thank our anonymous reviewer for useful and constrictive feedback.

This work made use of the excellent VizieR database of astronomical catalogues¹⁰ (Ochsenbein, Bauer & Marcout 2000).

REFERENCES

Asplund M., Grevesse N., Sauval A. J., 2005, in T. G. Barnes III & F. N. Bash ed., *Cosmic Abundances as Records of Stellar Evolution and Nucleosynthesis* Vol. 336

- of Astronomical Society of the Pacific Conference Series, The Solar Chemical Composition. pp 25–+
- Bacon R., et al., 2006, *The Messenger*, 124, 5, arXiv:astro-ph/0606329
- Becker G. D., Rauch M., Sargent W. L. W., 2009, *ApJ*, 698, 1010, arXiv:0812.2856
- Bolton J. S., Haehnelt M. G., 2007, *MNRAS*, 382, 325, arXiv:astro-ph/0703306
- Bouwens R. J., Illingworth G. D., Franx M., Ford H., 2007, *ApJ*, 670, 928, arXiv:0707.2080
- Bouwens R. J., Illingworth G. D., Franx M., Ford H., 2008, *ApJ*, 686, 230, arXiv:0803.0548
- Bouwens R. J., Illingworth G. D., Oesch P. A., Labbe I., Trenti M., van Dokkum P., Franx M., Stiavelli M., Carollo C. M., Magee D., Gonzalez V., 2010, *ArXiv e-prints*, arXiv:1006.4360
- Cen R., Chisari N. E., 2010, *ArXiv e-prints*, arXiv:1005.1451
- Chabrier G., 2003, *PASP*, 115, 763, arXiv:astro-ph/0304382
- Chary R., 2008, *ApJ*, 680, 32, arXiv:0712.1498
- Davé R., Oppenheimer B. D., 2007, *MNRAS*, 374, 427, arXiv:astro-ph/0608268
- Fox A. J., Ledoux C., Petitjean P., Srianand R., 2007, *A&A*, 473, 791, arXiv:0707.4065
- Gavilán M., Buell J. F., Mollá M., 2005, *A&A*, 432, 861, arXiv:astro-ph/0411746
- Hui L., Gnedin N. Y., 1997, *MNRAS*, 292, 27, arXiv:astro-ph/9612232
- Kennicutt Jr. R. C., 1998, *ARA&A*, 36, 189, arXiv:astro-ph/9807187
- Komatsu E., et al., 2010, *ArXiv e-prints*, arXiv:1001.4538
- Kroupa P., Tout C. A., Gilmore G., 1993, *MNRAS*, 262, 545
- Martin C. L., Scannapieco E., Ellison S. L., Hennawi J. F., Djorgovski S. G., Fournier A. P., 2010, *ApJ*, 721, 174, arXiv:1007.2457
- Mesinger A., 2010, *MNRAS*, 407, 1328, arXiv:0910.4161
- Ochsenbein F., Bauer P., Marcout J., 2000, *A&AS*, 143, 23, arXiv:astro-ph/0002122
- Oesch P. A., Carollo C. M., Stiavelli M., Trenti M., Bergeron L. E., Koekemoer A. M., Lucas R. A., Pavlovsky C. M., Beckwith S. V. W., Dahlen T., Ferguson H. C., Gardner J. P., Lilly S. J., Mobasher B., Panagia N., 2009, *ApJ*, 690, 1350, arXiv:0804.4874
- Omukai K., Schneider R., Haiman Z., 2008, *ApJ*, 686, 801, arXiv:0804.3141
- Oppenheimer B. D., Davé R., 2006, *MNRAS*, 373, 1265, arXiv:astro-ph/0605651
- Oppenheimer B. D., Davé R., 2008, *MNRAS*, 387, 577, arXiv:0712.1827
- Oppenheimer B. D., Davé R., Finlator K., 2009, *MNRAS*, 396, 729, arXiv:0901.0286
- Pawlik A. H., Schaye J., van Scherpenzeel E., 2009a, *ArXiv e-prints*, arXiv:0912.3034
- Pawlik A. H., Schaye J., van Scherpenzeel E., 2009b, *MNRAS*, 394, 1812, arXiv:0807.3963
- Pettini M., Madau P., Bolte M., Prochaska J. X., Ellison S. L., Fan X., 2003, *ApJ*, 594, 695, arXiv:astro-ph/0305413
- Rollinde E., Vangioni E., Maurin D., Olive K. A., Daigne F., Silk J., Vincent F. H., 2009, *MNRAS*, 398, 1782,

¹⁰ <http://vizier.u-strasbg.fr/>

- arXiv:0806.2663
- Romano D., Chiappini C., Matteucci F., Tosi M., 2005, *A&A*, 430, 491
- Romano D., Karakas A. I., Tosi M., Matteucci F., 2010, *ArXiv e-prints*, arXiv:1006.5863
- Ryan-Weber E. V., Pettini M., Madau P., Zych B. J., 2009, *MNRAS*, 395, 1476, arXiv:0902.1991
- Salvaterra R., Ferrara A., Dayal P., 2010, *ArXiv e-prints*, arXiv:1003.3873
- Schaerer D., 2002, *A&A*, 382, 28, arXiv:astro-ph/0110697
- Songaila A., 2001, *ApJ*, 561, L153, arXiv:astro-ph/0110123
- Songaila A., 2006, *AJ*, 131, 24, arXiv:astro-ph/0509821
- Steidel C. C., Erb D. K., Shapley A. E., Pettini M., Reddy N., Bogosavljević M., Rudie G. C., Rakic O., 2010, *ApJ*, 717, 289, arXiv:1003.0679
- Tilvi V., Rhoads J. E., Hibon P., Malhotra S., Wang J., Veilleux S., Swaters R., Probst R., Krug H., Finkelstein S. L., Dickinson M., 2010, *ApJ*, 721, 1853, arXiv:1006.3071
- Trac H., Cen R., 2007, *ApJ*, 671, 1, arXiv:astro-ph/0612406
- Tyson N. D., 1988, *ApJ*, 329, L57
- Tytler D., Gleed M., Melis C., Chapman A., Kirkman D., Lubin D., Paschos P., Jena T., Crotts A. P. S., 2009, *MNRAS*, 392, 1539
- van Dokkum P., Conroy C., 2010, *ArXiv e-prints*, arXiv:1009.5992
- Ventura P., Marigo P., 2010, *MNRAS*, pp 1247–+, arXiv:1007.2533
- Woolsey S. E., Weaver T. A., 1995, *ApJS*, 101, 181